ChemPubSoc Europe

DOI: 10.1002/open.201500109

Open Access ChemistryOPEN Full Papers

Gold Nanoparticles Decorated with Sialic Acid Terminated Bi-antennary N-Glycans for the Detection of Influenza Virus at Nanomolar Concentrations**

Vivek Poonthiyil,[a, b] Prashanth T. Nagesh,[d] Matloob Husain,[d] Vladimir B. Golovko,*[a, b] and Antony J. Fairbanks*[a, c]

Gold nanoparticles decorated with full-length sialic acid terminated complex bi-antennary N-glycans, synthesized with glycans isolated from egg yolk, were used as a sensor for the detection of both recombinant hemagglutinin (HA) and whole influenza A virus particles of the H1N1 subtype. Nanoparticle aggregation was induced by interaction between the sialic acid termini of the glycans attached to gold and the multivalent sialic acid binding sites of HA. Both dynamic light scattering (DLS) and UV/Vis spectroscopy demonstrated the efficiency of the sensor, which could detect viral HA at nanomolar concentrations and revealed a linear relationship between the extent of nanoparticle aggregation and the concentration of HA. UV/Vis studies also showed that these nanoparticles can selectively detect an influenza A virus strain that preferentially binds sialic acid terminated glycans with $\alpha(2\rightarrow6)$ linkages over a strain that prefers glycans with terminal $\alpha(2\rightarrow3)$-linked sialic acids.

Introduction

Constructs comprised of metal nanoparticles attached to a variety of chemical entities with specific binding properties have attracted significant interest in the fields of therapeutics,[1] diagnostics,[2] and sensing.[3] Gold nanoparticles (AuNPs) are particularly well suited to such applications for a number of reasons: there are well-established methods for the synthesis of AuNPs with defined sizes and shapes, it is easy to modify their surfaces, and they have excellent stability and biocompatibility.[4] In particular, interest in the application of modified AuNPs as colorimetric sensors has increased exponentially over the last two decades due to some of their unique properties, such as localized surface plasmon resonance (LSPR) and their high extinction coefficients.[5]

The distinctive color change of a AuNP solution in the presence of a specific analyte, upon either aggregation (red to purple/blue) or aggregate re-dispersion (purple/blue to red), makes AuNPs an ideal choice as a colorimetric sensor.[6] Such sensors based on AuNP aggregation have been used for a wide variety of analytes including low-molecular-weight species, such as metal ions, anions, amino acids and small-molecule pharmaceuticals, as well as larger species, such as peptides, proteins, DNA, and single cells.[7]

Dynamic light scattering (DLS, also known as photon correlation spectroscopy) is a noninvasive technique used to measure the size distribution of proteins, polymers, and nanoparticles.[8] AuNPs have strong light-scattering properties; for instance, a AuNP with a diameter of 60 nm has a light-scattering cross-section 200–300 times larger than that of a polystyrene bead of the same size, and is 4–5 orders of magnitude larger than that of a florescent dye, such as fluorescein.[9] DLS has therefore been extensively used as a means of detection of AuNPs as the basis of sensors for various analytes.[10]

The influenza virus is a respiratory pathogen and causes an acute febrile respiratory infection in humans and other mammals. Influenza causes regular seasonal epidemics and occasional pandemics in the human population.[11] Recent reports show that seasonal influenza epidemics result in ~300 000 human deaths annually.[12] The influenza virus particle contains two types of surface glycoprotein: neuraminidase (NA) and hemagglutinin (HA), and influenza A viruses are subtyped according to the variations of these two glycoproteins, for example as H1N1.[13] Viral HA is an integral membrane glycoprotein and has a trimeric binding pocket on the globular head of each monomer.[14] HA from the influenza virus is made up of ~556

[a] V. Poonthiyil, Dr. V. B. Golovko, Prof. A. J. Fairbanks
Department of Chemistry, University of Canterbury
Private Bag 4800, Christchurch 8140 (New Zealand)
E-mail: antony.fairbanks@canterbury.ac.nz
vladimir.golovko@canterbury.ac.nz

[b] V. Poonthiyil, Dr. V. B. Golovko
The MacDiarmid Institute for Advanced Materials and Nanotechnology
Wellington 6140 (New Zealand)

[c] Prof. A. J. Fairbanks
Biomolecular Interaction Centre, University of Canterbury
Private Bag 4800, Christchurch 8140 (New Zealand)

[d] P. T. Nagesh, M. Husain
Department of Microbiology and Immunology, University of Otago
PO Box 56, Dunedin 9054 (New Zealand)

[**] This article is part of the Virtual Special Issue "Carbohydrates in the 21st Century: Synthesis and Applications".

Supporting information for this article is available on the WWW under http://dx.doi.org/10.1002/open.201500109.

amino acids, and accounts for more than 80% of the envelope proteins of the virus.[11,15] One of the essential steps in influenza virus infection is binding of the viral particles to host cells,[16] a process mediated by specific interactions between the HA of the virus and sialic acid residues present on the host cell.[17] It has been found that human-adapted influenza viruses preferentially bind to sialylglycans with terminal $\alpha(2\rightarrow6)$ linkages.[16] Whilst the binding constant of HA for a single sialic acid residue is relatively weak ($10^3\ M^{-1}$), the binding constant between the multiple HAs of a viral particle with the multiple sialic acids present on a host cell has been estimated to be $10^{13}\ M^{-1}$.[18] Thus, a multivalent effect significantly increases binding and prevents dissociation of the virus from the host cell.[18b]

Glycogold nanoparticles (gAuNPs, that is, AuNPs attached to saccharides or glycoconjugates) have been used as sensors for various biomolecules and toxins,[19] including the detection of pathogenic agents such as bacteria and viruses.[20] Indeed, the detection of both the influenza virus itself and viral HA using gAuNPs was reported recently.[18b,21] The majority of previous studies have involved AuNPs decorated with synthetic oligosaccharides of various lengths that were terminated with sialic acid. Although none of these materials corresponded to full-length N-glycans typically found on the mammalian cell surface, their syntheses were nonetheless typically time-consuming, expensive, and logistically demanding.[18b,21b,d] Additionally, in the case where sialic acid itself was used as the ligand for gAuNPs,[20a] the selective detection of human-adapted influenza viruses that prefer $\alpha(2\rightarrow6)$-linked sialylglycans is not possible.

In this study we isolated a sialylglycopeptide (SGP, a sialic acid terminated bi-antennary complex-type N-glycan attached to a short peptide) from egg yolks, following an improved procedure recently reported by Huang and co-workers.[22] The SGP was converted into a thiol-terminated sialylglycan, which was then used for the development of a simple and rapid sialylglycan-capped gold nanoparticle (SG-gAuNP)-based sensor for HA and virus detection, using both UV/Vis spectroscopy and DLS. To our knowledge, this is the first report of the synthesis of gAuNPs decorated with naturally occurring full-length sialic acid terminated N-glycans and their application as sensors for HA and the influenza virus. Whilst UV/Vis spectroscopy allowed easy and rapid detection of HA by measuring the red shift of the LSPR band, DLS provided quantitative information on the size of the AuNP aggregates that were formed in the presence of HA.[23] UV/Vis studies also showed that these nanoparticles could selectively detect an influenza A virus that preferentially binds sialic acid terminated glycans with $\alpha(2\rightarrow6)$ linkages over an influenza virus that prefers glycans with terminal $\alpha(2\rightarrow3)$-linked sialic acids. The study reported herein opens a new avenue for the development of an easy-to-use, inexpensive, selective, highly sensitive, and rapid sensing platform for the detection of the influenza virus.

Results and Discussion

Extraction of SGP and conversion into a thiol

Extraction from 300 egg yolks, following the procedure of Huang and colleagues,[22] yielded 1.200 g of SGP **1** (Scheme 1). Incubation of **1** with pronase (from *Streptomyces griseus*) in Tris·HCl buffer (pH 7.5) at 37 °C then afforded the asparagine-linked complex bi-antennary N-glycan **2**.[24] Reaction of thioglycolic acid **3** with acetyl chloride and triethylamine in 1,4-dioxane afforded *S*-acetylthioacetic acid **4**.[25] Reaction of **4** with *N*-hydroxysuccinimide and dicyclohexylcarbodiimide (DCC) in THF gave the activated ester **5**,[26] which was then reacted with **2** in sodium phosphate buffer (pH 7.4) containing 20% acetonitrile to give thioacetate **6**. Deacetylation of **6** by treatment with hydroxylamine hydrochloride followed by air oxidation afforded disulfide **7**, which could typically be made on a multi-hundred-milligram scale.

Synthesis and characterization of SG-gAuNPs

Citrate-capped AuNPs (diameter, Ø: 12 nm) were synthesized by using the Turkevich reaction.[27] Ligand exchange with disulfide **7** then gave 12-nm-diameter SG-gAuNPs;[19c] ligand exchange is driven by the higher binding affinity of gold for a thiol than for citrate. The FTIR spectrum of the sialylglycan-capped SG-gNPs was similar to that of the free disulfide **7**, indicating both the removal of citrate and the successful incorporation of sialylglycans on the surface of the NPs (see Supporting Information Figures S5 and S6).[28] The particle sizes and size distributions (as demonstrated by TEM) and the UV/Vis absorption spectra of the AuNPs were essentially the same both before and after ligand exchange, indicating that the AuNP cores had not been affected. Analysis of the TEM images of the SG-gAuNPs (at least 200 particles were measured) revealed the particle sizes to be 12.1 ± 1.6 nm (Figure 1a). The absorption maximum of the SG-gAuNPs in the UV/Vis spectrum was at 523 nm (Figure S3), whilst ESI-MS also confirmed that the sialylglycan had been successfully incorporated into the SG-gAuNPs. The average molecular formula of the SG-gAuNPs was determined by TGA (Figure S8, Supporting Information) to be $Au_{54464}(C_{90}H_{14}N_8O_{65}S)_{12404}$, which was confirmed by elemental analysis.[29]

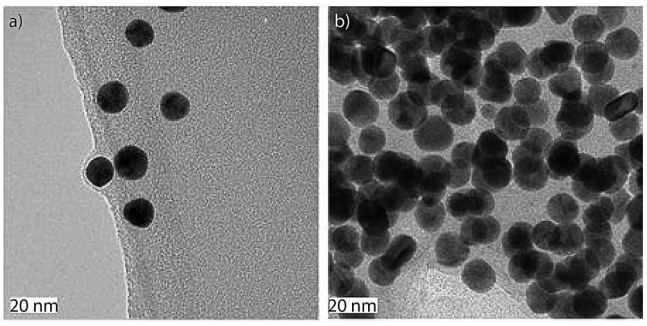

Figure 1. Representative TEM images of the SG-gAuNPs a) before and b) after the addition of HA.

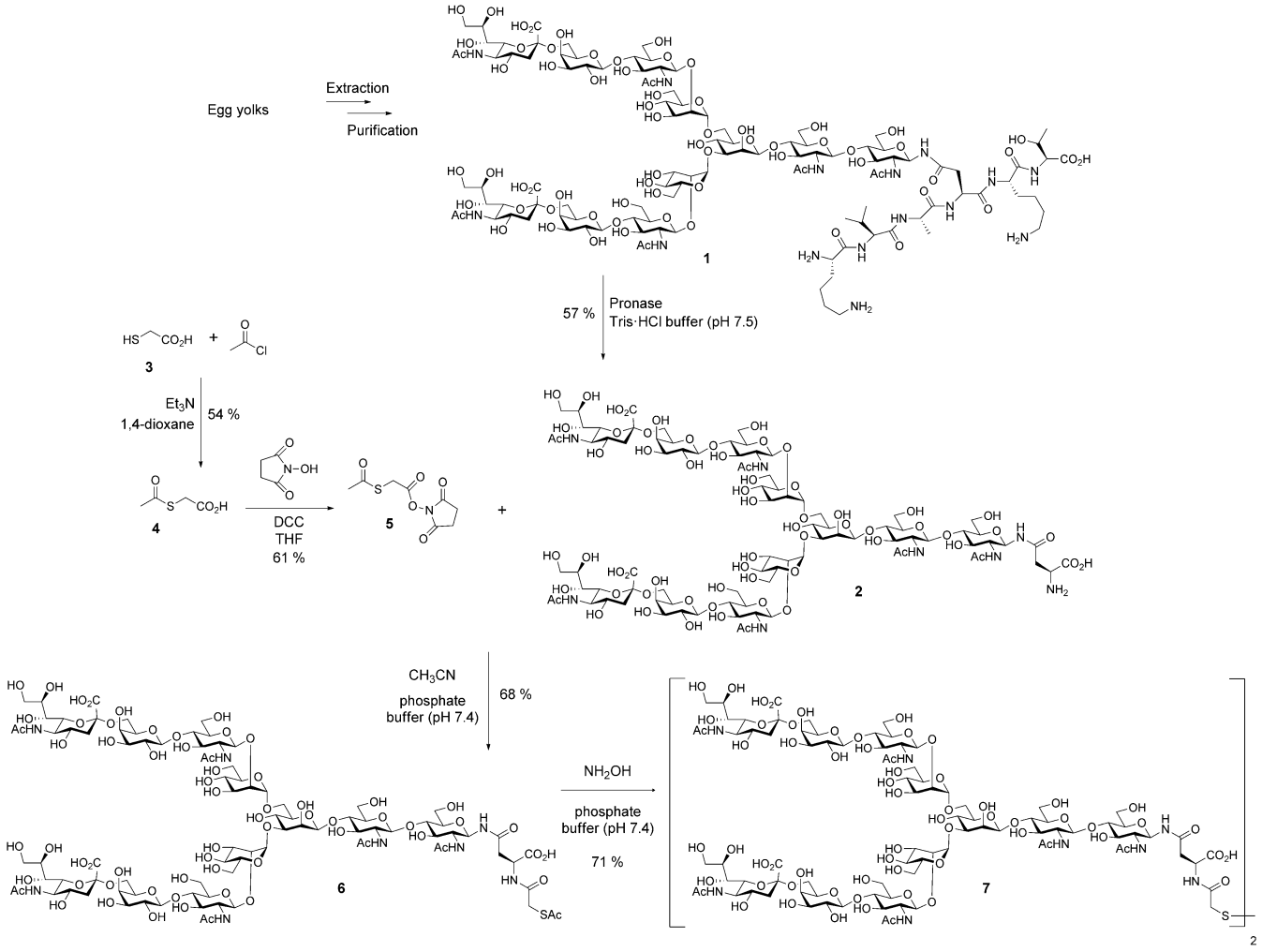

Scheme 1. Isolation and synthesis of the sialyloligosaccharide disulfide ligand **7**.

SG-gAuNP aggregation in the presence of HA

A pictorial representation of the HA-induced aggregation of SG-gAuNPs, based on previous reports on similar analyte-induced aggregation-effected sensors, is depicted in Figure 2.[6,21d] The performance of any gAuNP-based colorimetric sensing system depends on how effectively the gAuNP dispersion is converted into gAuNP aggregates by the analyte of interest. Typically, gAuNPs are stabilized against attractive van der Waals forces by the steric effects of the surface capping ligands: in this study, the sialic acid terminated complex bi-antennary N-glycans.[5a] Aggregation of gAuNPs can be achieved in two ways, either by inter-particle crosslinking or by non-crosslinking.[5a] Inter-particle crosslinking aggregation is presumed to be the basis of the sensing response reported here; controlled aggregation of the SG-gAuNPs occurs through binding of the multiple sialic acid binding sites of HA to the sialic acid terminated ligands present on the SG-gAuNPs.[16] Indeed the addition of excess sialic acid (10 mM) to a solution of SG-gAuNP aggregates formed in the presence of HA (564 nM) resulted in aggregate re-dispersion, as demonstrated by a color change (from blue to red) and by a blue-shift in the

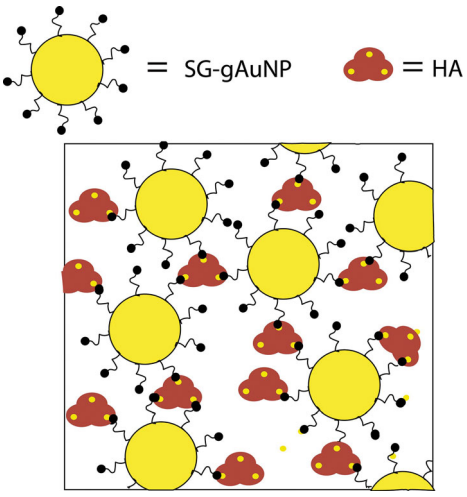

Figure 2. Schematic representation of the mechanism of aggregation of SG-gAuNPs in the presence of HA.

SPR peak maximum to $\lambda = 523$ nm. The dissociation of these aggregates to individual particles in the presence of sialic acid

showed that binding of the SG-gAuNPs to HA is reversible, and also provides strong supporting evidence for the mechanism of aggregation depicted in Figure 2. With respect to aggregation, TEM analysis also clearly showed that, following the addition of HA, the SG-gAuNPs were no longer present as individual well-separated particles (Figure 1a), but had assembled into networks of aggregated NPs (Figure 1b). HA detection was also possible simply with the naked eye, as the color of the colloidal solution changed from red to purple upon SG-gAuNP aggregation (Figure 3).

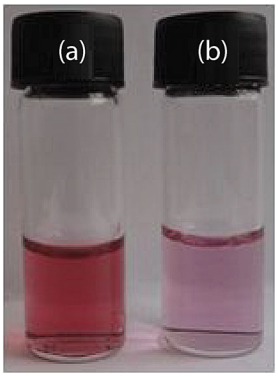

Figure 3. SG-gAuNP solutions a) before and b) after the addition of HA.

Colorimetric detection of influenza HA using SG-gAuNPs

When HA was added to the SG-gAuNPs (3 nM) to give a final HA concentration of 71 nM, the LSPR band peak maximum of SG-gAuNPs centered at $\lambda = 523$ nm did not undergo any significant shift, either immediately or upon standing (Figure S3, Supporting Information). However, when the final concentration of HA was increased to 141 nM, the SPR peak began to shift gradually in a time-dependent fashion, indicating aggregation of the SG-gAuNPs (Figure 4a). After 60 min no further change in the absorbance spectrum was observed, and the LSPR band peak maximum had shifted to $\lambda = 531$ nm. When the HA concentration was further increased to 283, 424, and 564 nM, the LSPR band peak maximum underwent even more pronounced shifts to 534, 539, and 544 nm, respectively, over the same time period (60 min), indicating the formation of progressively larger SG-gAuNP aggregates as the HA concentration was increased (Figure 4b–d).

A further demonstration of the effect of the HA concentration on the LSPR band of the SG-gAuNPs, by plotting the ratio of the absorbance intensity measured at $\lambda = 650$ nm both with and without HA $[(I^{HA}/I^{0})_{650}]$ against the HA concentration between 71 and 564 nM, is shown in Figure 5. These data show a linear relationship between the concentration of HA added and the degree of SG-gAuNP aggregation. This change in ab-

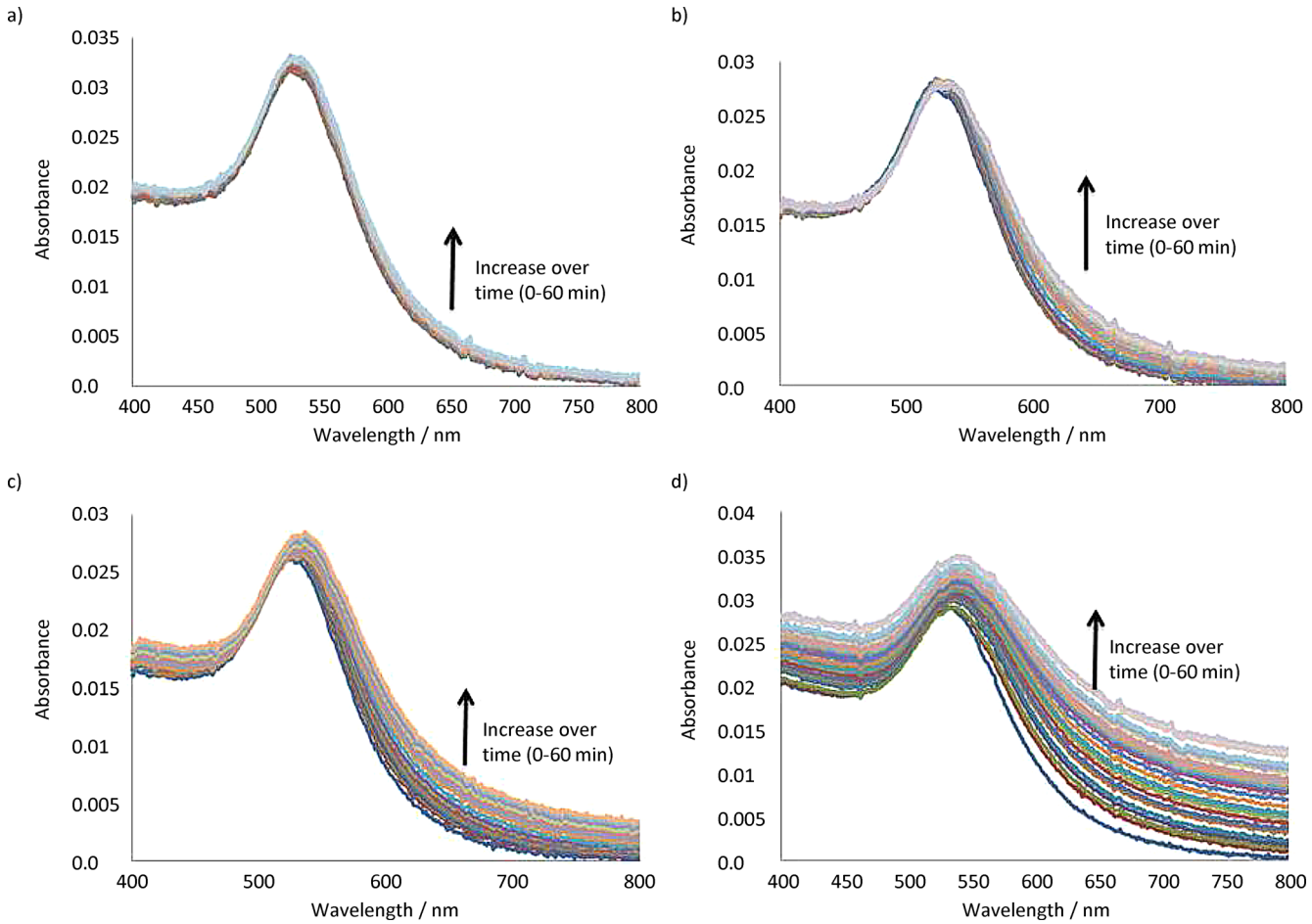

Figure 4. UV/Vis absorption spectra of SG-gAuNP with HA at concentrations of a) 141, b) 283, c) 424, and d) 564 nM.

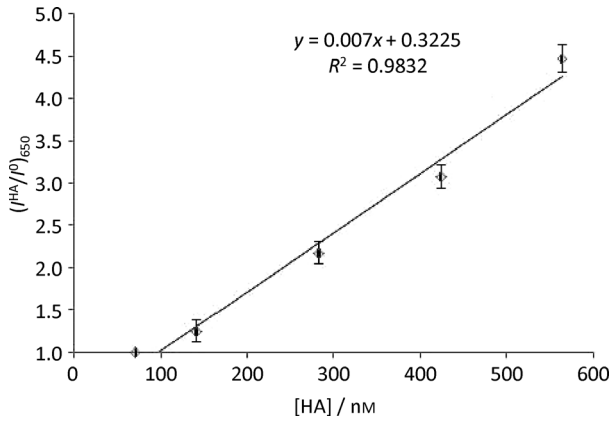

Figure 5. Plot of the ratio of absorbance intensity at 650 nm both with and without HA versus HA concentration for SG-gAuNP. Data points are the average ± SEM of three independent measurements.

sorbance can therefore be used to estimate the concentration of HA in an unknown sample. Wei et al.[21d] reported that at HA concentrations greater than 4.2 μg mL^{-1} (equivalent to 71 nM), AuNPs stabilized with synthetic mimics of sialylglycans were red shifted. Figure 5 demonstrates that the SG-gAuNPs reported here are similar in terms of detection efficiency, and that the sensitivity is similar to the results obtained from traditional methods such as ELISAs and glycan microarrays.[30] However, considering the logistically demanding and time-consuming chemoenzymatic synthetic procedure required to make the sialylglycan mimics in the report of Wei et al.,[21d] the use of naturally occurring full-length N-glycans reported herein offers a simpler and more attractive method for the development of an AuNP-based sensor for HA detection.

Colorimetric detection of the influenza virus

It is known that in general avian-adapted influenza A viruses prefer sialylglycans with α(2→3) linkages that are present in the intestinal epithelial cells of birds, whilst human-adapted influenza A viruses prefer α(2→6) linkages, which are commonly expressed in the upper respiratory tract of humans.[16] To investigate any selectivity of the SG-gAuNPs produced in this study, UV/Vis experiments were performed with influenza virus strains A/Puerto Rico/8/34 (H1N1) and A/New Caledonia/20/1999 (H1N1). The A/Puerto Rico/8/34 strain (hereafter referred as the Puerto Rico strain) specifically binds α(2→3)-linked sialylglycans,[31] whilst the influenza A/New Caledonia/20/1999 strain (hereafter referred as the New Caledonia strain) has specificity for α(2→6)-linked glycans.[32] Upon the addition of 10000 plaque-forming units (PFU) of the New Caledonia strain to the SG-gAuNPs (3 nM), there was a significant increase in the absorbance intensity at $\lambda = 650$ nm (Figure 6). However, addition of the Puerto Rico strain at the same PFU number (and also at 30000 PFU; data not shown) did not result any increase in the absorbance intensity at $\lambda = 650$ nm, confirming that the SG-gAuNPs selectively detected viral particles that have α(2→6) specificity (Figure 6).

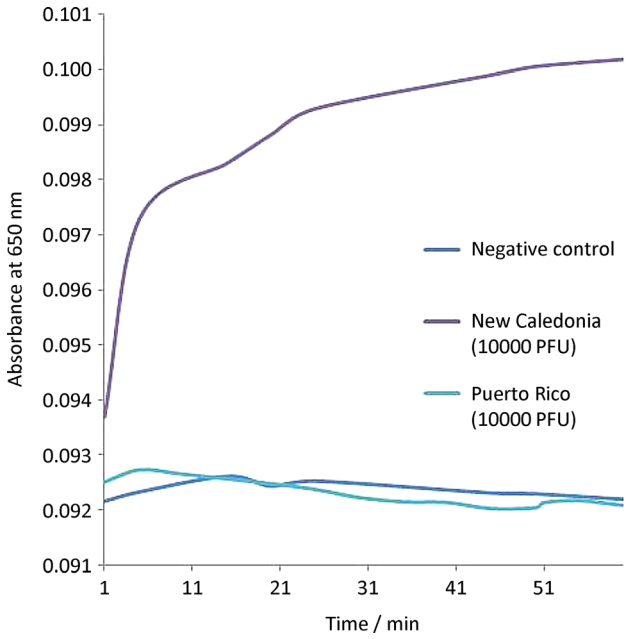

Figure 6. Plot of the absorbance intensity at 650 nm versus time for SG-gAuNPs with two different influenza virus strains as well as a negative control.

A further demonstration of the effect of the influenza virus concentration on the LSPR band of the SG-gAuNPs is shown in Figure 7, which plots the ratio of the absorbance intensity measured at $\lambda = 650$ nm both with and without the New Caledonia strain [$(I^{HA}/I^0)_{650}$] against the New Caledonia strain concentration between 1000 and 30000 PFU. These data show a linear relationship between the concentration of virus added and the degree of SG-gAuNP aggregation, which is similar to the case of HA shown in Figure 5. Additionally, the binding of the SG-gAuNPs to the virus was found to be faster than to HA. The virus–SG-gAuNP interaction was complete within 30 min, in line with the report of Wei et al.[21d] It is clear from Figure 7 that the SG-gAuNPs used here can readily detect the New Caledonia strain in amounts as low as 10000 PFU.

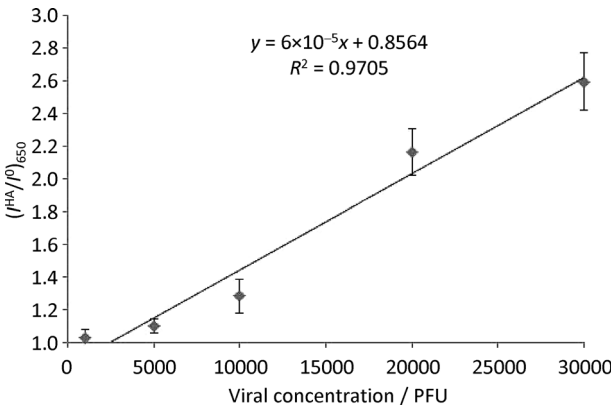

Figure 7. Plot of the ratio of the absorbance intensity at 650 nm with and without the New Caledonia strain versus the New Caledonia viral concentration. Data points are the average ± SEM of three independent measurements.

DLS detection of HA using SG-gAuNPs

The aggregation of SG-gAuNPs by the addition of varying concentrations of viral HA was also investigated by DLS, a technique that can provide a quantitative estimate of the average diameter of the AuNP aggregates produced.[33] As the ability of AuNPs to scatter light is significantly higher than that of biomolecules, DLS is selective for the AuNPs present in these solutions.[10a] In the DLS assays carried out in this study, the HA-induced SG-gAuNP aggregates were not physically separated from any remaining non-aggregated NPs that may have been present. However, the inherent bias of DLS toward larger particles and aggregates means that estimated diameters are representative of only the particle aggregates.[21c]

From the DLS measurements, the size of the "as made" SG-gAuNPs was found to be 21 ± 1 nm (Figure S4a, Supporting Information). The diameter of the AuNPs in solution measured by DLS is always larger than the AuNP core diameters measured by TEM[34] because organic ligands on the Au surface are transparent to electrons and so do not contribute to the size of the AuNPs when measured by TEM.[23] In contrast, DLS measures the hydrodynamic radius of the particles, which in this case includes the sialylglycan ligands and any trapped water molecules.[35]

When HA was added to SG-gAuNPs (3 nM) to obtain a final HA concentration of 71 nM, a DLS assay gave a particle size of 21 ± 1 nm, indicating that no aggregation had occurred at that HA concentration (Figure S4b, Supporting Information). All DLS measurements were carried out 60 min after the addition of HA to the SG-gAuNP solution, as after that point the LSPR band of the solutions remained constant. When the final HA concentration was increased to 141 nM, DLS indicated that the mean diameter of the SG-gAuNPs had increased to 97 ± 4 nm, clearly indicating aggregate formation in the presence of the HA at this concentration (Figure 8a). When the final HA concentration was further increased to 283, 424, and 564 nM, the mean diameters of the SG-gAuNP aggregates formed correspondingly increased to 183 ± 5, 389 ± 11, and 596 ± 21 nm respectively (Figure 8b–d). The larger standard deviation observed for the larger aggregates indicates that the polydispersity of the aggregates also increased with increasing HA concentration.

A plot of the size of SG-gAuNP aggregates measured by DLS versus HA concentration (Figure 9) was found to be linear, with an R^2 value of 0.9748. This linear relationship can therefore be used to estimate an unknown concentration of HA, in a similar fashion to the change in absorbance intensity at $\lambda = 650$ nm using UV/Vis (as shown in Figure 5). The proportionality constants of the two corresponding linear equations, 0.007 and 1.143 for the colorimetric and DLS assays respectively, indicate that the DLS assay is more sensitive toward nanoparticle aggregation, in accordance with previous reports.[8c, 36]

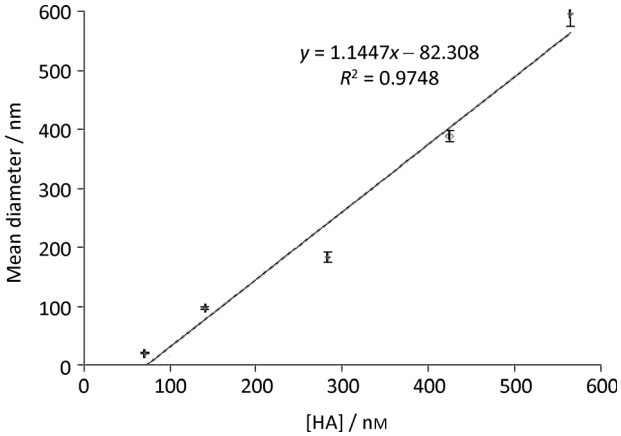

Figure 9. Plot of the SG-gAuNP aggregate size versus concentration of HA added. Data points are the average ± SEM of three independent measurements.

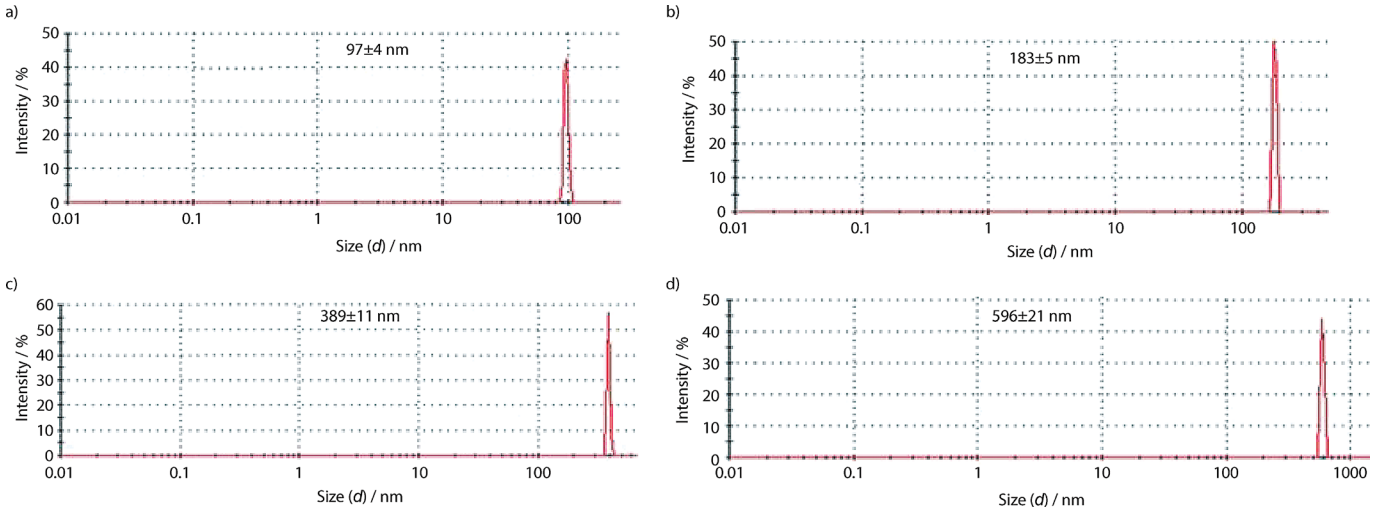

Figure 8. DLS measurements of the average diameters of the SG-gAuNP aggregates formed in the presence of HA at concentrations of a) 141, b) 283, c) 424, and d) 564 nM.

Selectivity of the SG-gAuNPs for HA

To demonstrate the selectivity of HA/virus detection by the SG-gAuNPs, aliquots of a SG-gAuNP solution were mixed with bovine serum albumin (BSA) and the lectins concanavalin A (Con A) and the B subunit of heat-labile enterotoxin (each at 600 nM). It was found that none of these species had any effect on either the UV/Vis absorption band or the DLS measurements, confirming that the SG-gAuNPs did not undergo nonspecific aggregation, and that amongst the species investigated detection was selective for HA and virus.

Conclusions

AuNPs capped with naturally occurring sialic acid terminated complex bi-antennary N-glycans can be used for the simple and highly selective detection of viral HA and the influenza virus, by the use of both DLS and UV/Vis spectroscopy. A homogeneous sialylglycopeptide, isolated from egg yolks by a simple procedure, was converted into a thiol and then used in a ligand-exchange reaction with citrate-capped AuNPs to obtain SG-gAuNPs. The presence of sialic acid binding sites on viral HA, and their specific and multivalent binding to sialic acid residues at the termini of the ligands on the SG-gAuNPs, caused nanoparticle aggregation as the basis for HA/virus detection. Both UV/Vis and DLS measurements revealed a linear relationship between SG-gAuNP aggregation and the concentration of HA that was added. Additionally, the SG-gAuNPs used in this study selectively detected viral particles with binding specificity for $\alpha(2\rightarrow6)$-linked sialylglycans. The SG-gAuNPs did not undergo nonspecific aggregation in the presence of BSA or two lectins. The SG-gAuNP-based sensor reported herein should allow the development of an easy-to-use, inexpensive, selective, and highly sensitive sensing platform for the detection of the influenza virus.

Experimental Section

Reagents: Water used throughout this study was purified by a Milli-Q system (Millipore). Au metal (99.99%), trisodium citrate, and concanavalin A (Con A) isolated from jack bean (*Canavalia ensifromis*) were purchased from Sigma–Aldrich. Recombinant influenza A virus H1N1 hemagglutinin (A/California/04/2009) was purchased from Sino Biological Inc. (Beijing, China). The influenza virus strains A/Puerto Rico/8/34 (H1N1) and A/New Caledonia/20/1999 (H1N1) were propagated in 10-day-old embryonated chicken eggs, and titrated on Madin–Darby canine kidney (MDCK) cells. The B-subunit of heat-labile enterotoxin was purchased from Reagent Proteins (San Diego, CA, USA). Tetrachloroauric(III) acid trihydrate ($HAuCl_4{\cdot}3H_2O$) was prepared following published procedures.[37] All other reagents and solvents were analytical grade and were used without further purification.

Instrumentation: Infrared spectra were recorded on a PerkinElmer Spectrum One instrument. ^{1}H NMR (δ_H) spectra were recorded on Agilent Technologies 400 MR (400 MHz) or Varian VNMR500 (500 MHz) spectrometers. All chemical shifts are quoted on the δ scale in ppm using residual solvent as internal standard. High-resolution mass spectra were recorded with a BrukermaXis 3G UHR-TOF mass spectrometer. Thermogravimetric analysis (TGA) was performed with an Alphatech SDT Q600 TGA/DSC apparatus on 6–8 mg of purified dry materials (alumina crucible was used as the sample holder), under N_2 (at a flow rate of 100 mL min^{-1}), recording data from 25 to 1000 °C at a heating rate of 10 °C min^{-1}. Elemental analyses were performed by the Campbell Microanalytical Laboratory at the University of Otago. TEM images of AuNPs were obtained using a Philips CM200 TEM operating at 200 kV. Samples for TEM imaging were prepared by dropping 2 μL of a freshly prepared solution of nanostructured Au onto a holey carbon-coated copper grid (300 mesh, SPI Supplies, USA) followed by drying at room temperature. UV/Vis absorption spectra were recorded with a Varian Cary 100 UV/Vis spectrophotometer or a multimode reader (Varioskan Flash, Thermo Scientific). DLS measurements were performed using a Malvern Zetasizer Nano ZS DLS system (Malvern Instruments Ltd., UK). The DLS system is equipped with a $\lambda = 633$ nm He–Ne laser and an avalanche photodiode detector configured to collect backscattered light at 173°.

Colorimetric detection of HA using SG-gAuNPs: Purified SG-gAuNPs were freeze-dried and then re-suspended in PBS (pH 7.4) to give a nanoparticle concentration of 3 nM. A solution of HA in PBS (0.25 mg mL^{-1}, pH 7.4) was prepared. Aliquots of the HA solution (5, 10, 20, 30 and 40 μL) were then added (with mixing) to an aliquot of the SG-gAuNP solution (200 μL), and in each case the solution was made up to a total volume of 300 μL by adding PBS; reaction progress was monitored by UV/Vis spectroscopy at various time intervals. Additionally, an aliquot of the SG-gAuNP solution (200 μL) was also mixed with BSA (600 nM) to confirm that the SG-gAuNPs did not undergo nonspecific aggregation, and also with Con A and B subunits of heat-labile enterotoxin (each at 600 nM) to confirm that the particles were selective only toward HA.

Colorimetric detection of viral particles using SG-gAuNPs: Egg allantoic fluid containing influenza strains A/New Caledonia/20/1999 (H1N1; 6×10^5 PFU mL^{-1}) or A/Puerto Rico/8/34 (H1N1; 2×10^7 PFU mL^{-1}) was prepared in PBS. Aliquots of the A/New Caledonia/20/1999 (H1N1) solution (1.6, 8.0, 16.7, 33.4, and 50.1 μL) were added (with mixing) to an aliquot of the SG-gAuNP solution (30 μL of 20 nM solution) and formalin (15 μL of 10% stock solution). In each case, the solution was made up to a total volume of 300 μL by adding PBS. Reaction progress was monitored by UV/Vis spectroscopy at various time intervals. In the case of the A/Puerto Rico/8/34 (H1N1) virus, 1.5 μL of the stock solution was added to the SG-AuNP solution.

DLS assay: The sample was equilibrated at 25 °C for 120 s before analysis. Each measurement consisted of 12 scans, each 30 s in duration. The mean particle hydrodynamic diameters reported were calculated from intensity-based particle size distributions.

Extraction of sialylglycopeptide (SGP) from egg yolks 1:[22] Egg yolks (300 total, 3.3 L) were stirred in H_2O (1.5 L) and then freeze-dried to obtain 2.1 kg of yolk powder. This powder was washed successively with Et_2O (2×6 L) and 70% aqueous acetone (6 L) after thorough mixing. Aqueous acetone (40%, 2×3 L) was added with vigorous mixing, and the solution was then filtered through Celite. The filtrate was concentrated and freeze-dried to give 30 g of yolk extract powder. This powder (30 g) was dissolved in H_2O and purified by solid-phase extraction with an active carbon/Celite (300 g:300 g) column (the column was sequentially washed with 5% and 10% aqueous CH_3CN before elution of SGP with 30% aqueous CH_3CN) to afford 1.2 g of sialylglycopeptide (SGP) **1**[22] as a white powder. ^{1}H NMR (400 MHz, D_2O): $\delta = 0.84$ (6H, d, γCH_3 of Val), 1.04 (3H, d, γCH_3 of Thr), 1.25 (3H, d, βCH_3 of Ala), 1.31 (2H,

m, γCH_2 of Lys), 1.52–1.64 (3H, m, δCH_2 of Lys, H-3_{ax} NeuAc7, H-3_{ax} NeuAc7′), 1.75 (2H, m, βCH_2 of Lys), 2.54 (1H, m, H-3_{eq} NeuAc7, H-3_{eq} NeuAc7′), 2.70 (2H, m, βCH_2 of Asn), 2.87 (2H, t, εCH_2 of Lys), 4.33 (2H, d, H-1Gal-6, H-1Gal6′), 4.47 (3H, m, H-1GlcNAc2, H-1GlcNAc5, H-1GlcNAc5′), 4.63 (1H, m, H-1Man3), 4.82 (1H, m, H-1Man4′), 4.91 (1H, d, H-1GlcNAc1), 5.00 (1H, m, H-1Man4); HRMS (ESI): calcd for $C_{112}H_{189}N_{15}O_{70}$ $[M+H]^+$ 2865.1764, found 2865.1734.

Asparagine-linked complex bi-antennary N-glycan 2:[24] Pronase (3 mg, from *Streptomyces griseus*) was added to a solution of SGP **1**[22] (20 mg) and NaN_3 in Tris·HCl buffer (50 mM, pH 7.5, 1 mL), and the mixture was incubated at 37 °C. The pH of the solution was checked regularly and adjusted to 7.5. After seven days, the mixture was purified by gel filtration using a Sephadex G-25 column (8.7×1.7 cm) which was pre-equilibrated and eluted with 0.01% aqueous NH_3. Fractions (8 mL) were collected at a flow rate of 0.5 mL min^{-1} and examined for their sugar content using the phenol/H_2SO_4 test. The fractions that showed positive results were pooled and lyophilized to obtain asparagine-linked N-glycan **2**[24] (10 mg, 57%) as a white powder. ^{1}H NMR (400 MHz, D_2O): δ = 1.80 (2H, at, *J* = 12.4 Hz, H-3_{ax} NeuAc7, H-3_{ax} NeuAc7′), 2.10–2.2 (18H, s, 6×CH_3CO_2), 2.76 (2H, m, H-3_{eq} NeuAc7, H-3_{eq} NeuAc7′), 2.95 (1H, dd, *J* = 8, 16 Hz, βCH_2 of Asn), 3.03 (1H, dd, *J* = 4, 16 Hz, βCH_2 of Asn), 4.17 (1H, bd, H-2Man4′), 4.24 (1H, bd, H-2Man4), 4.30 (1H, bs, H-2Man3), 4.49 (2H, d, *J* = 7.6 Hz, H-1Gal6, H-1Gal6′), 4.66 (3H, m, H-1GlcNAc2, H-1GlcNAc5, H-1GlcNAc5′), 4.86 (1H, s, H-1Man3), 5.15 (1H, d, *J* = 9.5 Hz, H-1GlcNAc), 5.18 (1H, s, H-1Man4); HRMS (ESI) calcd for $C_{88}H_{144}N_8O_{64}$ $[M+H]^+$ 2337.8390, found 2337.8340.

***S*-Acetylthioacetic acid 4**:[25] Acetyl chloride (3.8 mL, 0.054 mmol) was added dropwise to a stirred mixture of Et_3N (15 mL, 0.108 mol) and thioglycolic acid **3** (5.22 g, 0.054 mol) in 1,4-dioxane (100 mL) at 0 °C under N_2, and the reaction was then warmed to room temperature. After 12 h, TLC (EtOAc) showed the formation of a major product (R_f = 0) and the complete consumption of starting material (R_f = 0.5). The reaction mixture was filtered through Celite and concentrated in vacuo. Aqueous HCl (1 M, 30 mL) was added, and the reaction was stirred for 1 h. The reaction mixture was extracted with CH_2Cl_2 (3×30 mL), dried ($MgSO_4$), filtered, and concentrated in vacuo to give *S*-acetylthioacetic acid **4**[25] (4.2 g, 54%) as a yellow oil. ^{1}H NMR (400 MHz, CD_3SOCD_3): δ = 2.35 (3H, s, CH_3COS), 3.66 (2H, s, CH_2CO_2), 12.75 (1H, br s, COOH).

***N*-Hydroxysuccinimide ester 5**:[26] *S*-Acetylthioacetic acid **4**[25] (2.6 g, 0.019 mol) and *N*-hydroxysuccinimide (2.2 g, 0.019 mol) were dissolved in THF (50 mL), and the reaction mixture was stirred at room temperature for 10 min before cooling to 0 °C. Dicyclohexylcarbodiimide (DCC; 3.97 g, 0.019 mol) was dissolved in THF (5 mL) and then added to the reaction mixture. The reaction mixture was warmed to room temperature and stirred under N_2. After 12 h, TLC (EtOAc/MeOH 4:1) showed the formation of a major product (R_f = 0.6) and the complete consumption of starting material (R_f = 0.4). The residue was purified by flash column chromatography (PE/EtOAc 2:1) to afford *N*-hydroxysuccinimide ester **5**[26] (1.9 g, 61%) as a yellow oil. ^{1}H NMR (400 MHz, CD_3Cl_3):[26] δ = 2.43 (3H, s, $COCH_3$), 2.85 (4H, s, $C(O)CH_2CH_2CO$), 3.99 (2H, s, SCH_2CO_2).

Thioacetate 6: A solution of *N*-hydroxysuccinimide ester **5**[26] (12 mg, 0.049 mmol) in CH_3CN (0.3 mL) was added to a solution of asparagine-linked N-glycan **2**[24] (7.6 mg, 0.003 mmol) in sodium phosphate buffer (50 mM, 1 mL, pH 7.4) containing 20% CH_3CN. The mixture was stirred at room temperature for 12 h and then lyophilized. The residue was purified by gel filtration on a Sephadex G-25 column (8.7×1.7 cm), which was pre-equilibrated and eluted with 0.01% aqueous NH_3 to obtain thioacetate **6** (5 mg, 68%) as a white powder. ^{1}H NMR (400 MHz, D_2O): δ = 1.80 (2H, at, *J* = 12.4 Hz, H-3_{ax} NeuAc7, H-3_{ax} NeuAc7′), 2.10–2.2 (18H, s, 6×CH_3CO_2), 2.30 (3H, s, CH_3COS), 2.53–2.67 (4H, m, βCH_2 of Asn, H-3_{eq} NeuAc7, H-3_{eq} NeuAc7′), 4.17 (1H, bd, H-2Man4′), 4.24 (1H, bd, H-2Man4), 4.30 (1H, bs, H-2Man3), 4.49 (2H, d, *J* = 7.6 Hz, H-1Gal6, H-1Gal6′), 4.66 (3H, m, H-1GlcNAc2, H-1GlcNAc5, H-1GlcNAc5′), 4.86 (1H, s, H-1Man3), 5.15 (1H, d, *J* = 9.5 Hz, H-1GlcNAc), 5.18 (1H, s, H-1Man4); HRMS (ESI) calcd for $C_{92}H_{148}N_8O_{66}S$ $[M+H]^+$ 2453.8264, found 2453.8191.

Disulfide 7: Hydroxylamine hydrochloride (51 mg, 0.73 mmol) was added to a solution of thioacetate **6** (300 mg, 0.122 mmol) in sodium phosphate buffer (100 mM, 80 mL, pH 7.4). The mixture was stirred at room temperature for 2 h and then lyophilized. The residue was purified by gel filtration on a Sephadex G-25 column (8.7×1.7 cm), which was pre-equilibrated and eluted with 0.01% aqueous NH_3 followed with oxidation by bubbling air continuously through the solution for a total of 64 h to obtain sialylglycan disulfide **7** (210 mg, 71%) as a white powder. ^{1}H NMR (400 MHz, D_2O): δ = 1.80 (2H, at, *J* = 12.4 Hz, H-3_{ax} NeuAc7, H-3_{ax} NeuAc7′), 2.10–2.2 (18H, s, 6×CH_3CO_2), 2.53–2.67 (4H, m, βCH_2 of Asn, H-3_{eq} NeuAc7, H-3_{eq} NeuAc7′), 4.17 (1H, bd, H-2Man4′), 4.24 (1H, bd, H-2Man4), 4.30 (1H, bs, H-2Man3), 4.49 (2H, d, *J* = 7.6 Hz, H-1Gal6, H-1Gal6′), 4.66 (3H, m, H-1GlcNAc2, H-1GlcNAc5, H-1GlcNAc5′), 4.86 (1H, s, H-1Man3), 5.15 (1H, d, *J* = 9.5 Hz, H-1GlcNAc), 5.18 (1H, s, H-1Man4); HRMS (ESI) calcd for $C_{90}H_{146}N_8O_{65}S$ $[M+2H]^{2+}$ 1205.9082, found 1205.9192.

Sialylglycan-capped gold nanoparticles (SG-gAuNP): An aqueous solution of trisodium citrate (1.7 mL, 39.0 mM) was added to a boiling aqueous solution of tetrachloroauric acid (7.6 mL, 1 mM) with constant stirring (500 rpm). After 15 min, the reaction mixture was cooled to room temperature, and a solution of disulfide **7** (144 mg, 1 mmol) was added. The reaction was stirred for 48 h at RT. The reaction mixture was concentrated in vacuo, the residue was dissolved in Milli-Q H_2O (10 mL), and then purified by centrifugal filtering (Amicon Ultra 10K, Millipore, MWCO = 10 kDa, 1 h, 5000 *g*). The residue was then dissolved in H_2O (2 mL) and lyophilized to obtain SG-gAuNP. TEM: Ø = 12.1 ± 1.6 nm; IR (KBr): $\tilde{\nu}$ = 3300 (broad band), 2933, 2873, 1062 cm^{-1}; UV: 523 nm; TGA: ligand 73.6%, Au 26.4%; Elemental analysis: found C 32.65, H 4.50, N 3.44, S 1.04, calcd for $Au_{54464}(C_{12}H_{24}O_8S)_{12404}$: C 32.96, H 4.47, N 3.42, S 1.01%; HRMS (ESI) calcd for $C_{90}H_{146}N_8O_{66}S$ $[M+2H]^{2+}$ 1206.4116, found 1206.415.

Acknowledgements

The authors thank Dr. Yusuke Tomabechi, Professor Milo Kral, Mike Flaws (TEM), Alistair Duff (AAS), and Rayleen Fredericks (DLS) for technical assistance. Financial support is gratefully acknowledged from the University of Canterbury (PhD scholarship to V.P.), the University of Otago (PhD scholarship to P.T.N.), the Health Research Council (Emerging Researcher Grant 12/614 to M.H.), and the MacDiarmid Institute.

Keywords: carbohydrates · gold nanoparticles · hemagglutinin · influenza · sensors · sialylglycan

[1] E. Boisselier, D. Astruc, *Chem. Soc. Rev.* **2009**, *38*, 1759–1782.
[2] R. Wilson, *Chem. Soc. Rev.* **2008**, *37*, 2028–2045.

[3] a) M. De, P. S. Ghosh, V. M. Rotello, *Adv. Mater.* **2008**, *20*, 4225 – 4241; b) I. Willner, R. Baron, B. Willner, *Biosens. Bioelectron.* **2007**, *22*, 1841 – 1852.
[4] a) Z. Wang, L. Ma, *Coord. Chem. Rev.* **2009**, *253*, 1607 – 1618; b) R. Sardar, A. M. Funston, P. Mulvaney, R. W. Murray, *Langmuir* **2009**, *25*, 13840 – 13851; c) R. A. Sperling, P. Rivera Gil, F. Zhang, M. Zanella, W. J. Parak, *Chem. Soc. Rev.* **2008**, *37*, 1896 – 1908; d) J. N. Anker, W. P. Hall, O. Lyandres, N. C. Shah, J. Zhao, R. P. Van Duyne, *Nat. Mater.* **2008**, *7*, 442 – 453; e) P. K. Jain, X. Huang, I. H. El-Sayed, M. A. El-Sayed, *Acc. Chem. Res.* **2008**, *41*, 1578 – 1586.
[5] a) W. Zhao, M. A. Brook, Y. Li, *ChemBioChem* **2008**, *9*, 2363 – 2371; b) V. Poonthiyil, V. B. Golovko, A. J. Fairbanks, *Org. Biomol. Chem.* **2015**, *13*, 5215 – 5223.
[6] M. J. Marín, C. L. Schofield, R. A. Field, D. A. Russell, *Analyst* **2015**, *140*, 59 – 70.
[7] K. Saha, S. S. Agasti, C. Kim, X. Li, V. M. Rotello, *Chem. Rev.* **2012**, *112*, 2739 – 2779.
[8] a) Q. Dai, X. Liu, J. Coutts, L. Austin, Q. Huo, *J. Am. Chem. Soc.* **2008**, *130*, 8138 – 8139; b) B. I. Ipe, A. Shukla, H. Lu, B. Zou, H. Rehage, C. M. Niemeyer, *ChemPhysChem* **2006**, *7*, 1112 – 1118; c) J. R. Kalluri, T. Arbneshi, S. Afrin Khan, A. Neely, P. Candice, B. Varisli, M. Washington, S. McAfee, B. Robinson, S. Banerjee, A. K. Singh, D. Senapati, P. C. Ray, *Angew. Chem. Int. Ed.* **2009**, *48*, 9668 – 9671; *Angew. Chem.* **2009**, *121*, 9848 – 9851.
[9] a) P. K. Jain, K. S. Lee, I. H. El-Sayed, M. A. El-Sayed, *J. Phys. Chem. B* **2006**, *110*, 7238 – 7248; b) J. Yguerabide, E. E. Yguerabide, *Anal. Biochem.* **1998**, *262*, 137 – 156; c) H. Jans, X. Liu, L. Austin, G. Maes, Q. Huo, *Anal. Chem.* **2009**, *81*, 9425 – 9432.
[10] a) H. Jans, Q. Huo, *Chem. Soc. Rev.* **2012**, *41*, 2849 – 2866; b) B.-A. Du, Z.-P. Li, C.-H. Liu, *Angew. Chem. Int. Ed.* **2006**, *45*, 8022 – 8025; *Angew. Chem.* **2006**, *118*, 8190 – 8193.
[11] K. Awazu, M. Fujimaki, S. C. Gopinath, *Sensors, 2013 IEEE*, November 3 – 6, 2013, Baltimore, MD (USA), pp. 1 – 3; DOI: 10.1109/ICSENS.2013.6688224.
[12] X. Li, P. Wu, G. F. Gao, S. Cheng, *Biomacromolecules* **2011**, *12*, 3962 – 3969.
[13] G. Neumann, T. Noda, Y. Kawaoka, *Nature* **2009**, *459*, 931 – 939.
[14] K. Subbarao, J. Katz, *Cell. Mol. Life Sci.* **2000**, *57*, 1770 – 1784.
[15] S. C. Gopinath, K. Awazu, M. Fujimaki, *Anal. Methods* **2010**, *2*, 1880 – 1884.
[16] M. Imai, Y. Kawaoka, *Curr. Opin. Virol.* **2012**, *2*, 160 – 167.
[17] N. K. Sauter, J. E. Hanson, G. D. Glick, J. H. Brown, R. L. Crowther, S. J. Park, J. J. Skehel, D. C. Wiley, *Biochemistry* **1992**, *31*, 9609 – 9621.
[18] a) M. Mammen, S.-K. Choi, G. M. Whitesides, *Angew. Chem. Int. Ed.* **1998**, *37*, 2754 – 2794; *Angew. Chem.* **1998**, *110*, 2908 – 2953; b) I. Papp, C. Sieben, K. Ludwig, M. Roskamp, C. Böttcher, S. Schlecht, A. Herrmann, R. Haag, *Small* **2010**, *6*, 2900 – 2906.
[19] a) J. de La Fuente, A. Barrientos, T. Rojas, J. Rojo, J. Canada, A. Fernandez, S. Penades, *Angew. Chem. Int. Ed.* **2001**, *40*, 2257; *Angew. Chem.* **2001**, *113*, 2317; b) M. Marradi, M. Martin-Lomas, S. Penadés, *Adv. Carbohydr. Chem. Biochem.* **2010**, *64*, 211 – 290; c) D. C. Hone, A. H. Haines, D. A. Russell, *Langmuir* **2003**, *19*, 7141 – 7144; d) C. L. Schofield, B. Mukhopadhyay, S. M. Hardy, M. B. McDonnell, R. A. Field, D. A. Russell, *Analyst* **2008**, *133*, 626 – 634; e) H. Otsuka, Y. Akiyama, Y. Nagasaki, K. Kataoka, *J. Am. Chem. Soc.* **2001**, *123*, 8226 – 8230; f) C. L. Schofield, R. A. Field, D. A. Russell, *Anal. Chem.* **2007**, *79*, 1356 – 1361.
[20] a) S.-J. Richards, E. Fullam, G. S. Besra, M. I. Gibson, *J. Mater. Chem. B* **2014**, *2*, 1490 – 1498; b) C.-C. Lin, Y.-C. Yeh, C.-Y. Yang, C.-L. Chen, G.-F. Chen, C.-C. Chen, Y.-C. Wu, *J. Am. Chem. Soc.* **2002**, *124*, 3508 – 3509; c) K. Niikura, K. Nagakawa, N. Ohtake, T. Suzuki, Y. Matsuo, H. Sawa, K. Ijiro, *Bioconjugate Chem.* **2009**, *20*, 1848 – 1852.
[21] a) C. Lee, M. A. Gaston, A. A. Weiss, P. Zhang, *Biosens. Bioelectron.* **2013**, *42*, 236 – 241; b) M. J. Marín, A. Rashid, M. Rejzek, S. A. Fairhurst, S. A. Wharton, S. R. Martin, J. W. McCauley, T. Wileman, R. A. Field, D. A. Russell, *Org. Biomol. Chem.* **2013**, *11*, 7101 – 7107; c) J. D. Driskell, C. A. Jones, S. M. Tompkins, R. A. Tripp, *Analyst* **2011**, *136*, 3083 – 3090; d) J. Wei, L. Zheng, X. Lv, Y. Bi, W. Chen, W. Zhang, Y. Shi, L. Zhao, X. Sun, F. Wang, *ACS Nano* **2014**, *8*, 4600 – 4607.
[22] B. Sun, W. Bao, X. Tian, M. Li, H. Liu, J. Dong, W. Huang, *Carbohydr. Res.* **2014**, *396*, 62 – 69.
[23] K. G. Witten, J. C. Bretschneider, T. Eckert, W. Richtering, U. Simon, *Phys. Chem. Chem. Phys.* **2008**, *10*, 1870 – 1875.
[24] N. Yamamoto, Y. Ohmori, T. Sakakibara, K. Sasaki, L. R. Juneja, Y. Kajihara, *Angew. Chem. Int. Ed.* **2003**, *42*, 2537 – 2540; *Angew. Chem.* **2003**, *115*, 2641 – 2644.
[25] D. N. Deaton, E. N. Gao, K. P. Graham, J. W. Gross, A. B. Miller, J. M. Strelow, *Bioorg. Med. Chem. Lett.* **2008**, *18*, 732 – 737.
[26] H. Saji, Y. Magata, Y. Arano, N. Yamamura (Nihon Medi-Physics Co., Ltd., Tokyo, Japan), European Patent No. EP1046401 A2, **2000**.
[27] G. Frens, *Nature Phys. Sci.* **1973**, *241*, 20.
[28] S.-Y. Lin, S.-W. Liu, C.-M. Lin, C.-h. Chen, *Anal. Chem.* **2002**, *74*, 330 – 335.
[29] a) K. Huang, H. Ma, J. Liu, S. Huo, A. Kumar, T. Wei, X. Zhang, S. Jin, Y. Gan, P. C. Wang, *ACS nano* **2012**, *6*, 4483 – 4493; b) Á. G. Barrientos, J. M. De La Fuente, T. C. Rojas, A. Fernández, S. Penadés, *Chem. Eur. J.* **2003**, *9*, 1909 – 1921.
[30] a) R. Xu, R. McBride, C. M. Nycholat, J. C. Paulson, I. A. Wilson, *J. Virol.* **2012**, *86*, 982 – 990; b) J. Stevens, O. Blixt, L. Glaser, J. K. Taubenberger, P. Palese, J. C. Paulson, I. A. Wilson, *J. Mol. Biol.* **2006**, *355*, 1143 – 1155; c) A. Chandrasekaran, A. Srinivasan, R. Raman, K. Viswanathan, S. Raguram, T. M. Tumpey, V. Sasisekharan, R. Sasisekharan, *Nat. Biotechnol.* **2008**, *26*, 107 – 113.
[31] C.-T. Guo, N. Takahashi, H. Yagi, K. Kato, T. Takahashi, S.-Q. Yi, Y. Chen, T. Ito, K. Otsuki, H. Kida, *Glycobiology* **2007**, *17*, 713 – 724.
[32] L.-M. Chen, P. Rivailler, J. Hossain, P. Carney, A. Balish, I. Perry, C. T. Davis, R. Garten, B. Shu, X. Xu, *Virology* **2011**, *412*, 401 – 410.
[33] X. Wang, O. Ramström, M. Yan, *Analyst* **2011**, *136*, 4174 – 4178.
[34] P. Ahonen, T. Laaksonen, A. Nykänen, J. Ruokolainen, K. Kontturi, *J. Phys. Chem. B* **2006**, *110*, 12954 – 12958.
[35] S. Diegoli, A. L. Manciulea, S. Begum, I. P. Jones, J. R. Lead, J. A. Preece, *Sci. Total Environ.* **2008**, *402*, 51 – 61.
[36] S. S. Dasary, D. Senapati, A. K. Singh, Y. Anjaneyulu, H. Yu, P. C. Ray, *ACS Appl. Mater. Interfaces* **2010**, *2*, 3455 – 3460.
[37] J. Brawer, *Handbook of Preparative Inorganic Chemistry, Vol. 1*, Academic Press, New York, **1963**.

Received: April 20, 2015
Published online on ■■ ■■, 0000

V. Poonthiyil, P. T. Nagesh, M. Husain, V. B. Golovko, A. J. Fairbanks**

■■ – ■■

Gold Nanoparticles Decorated with Sialic Acid Terminated Bi-antennary N-Glycans for the Detection of Influenza Virus at Nanomolar Concentrations

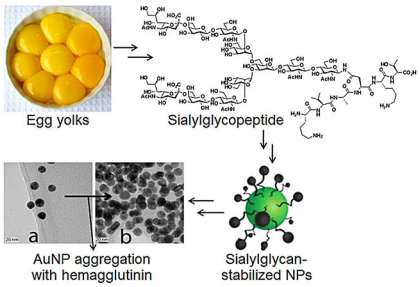

A golden egg yolk sensor: Full-length sialic acid terminated complex bi-antennary N-glycans, isolated from egg yolks, were used to develop glycogold nanoparticles for the colorimetric and dynamic light scattering detection of influenza virus particles and hemagglutinin. Particle sensing was selective for a virus strain that binds $\alpha(2\rightarrow6)$-linked sialic acid terminated glycans.

